

Phosphonium-Based Layered Silicate—Poly(ethylene terephthalate) Nanocomposites: Stability, Thermal and Mechanical Properties

T. Umasankar Patro, Devang V. Khakhar, Ashok Misra

Department of Chemical Engineering, Indian Institute of Technology Bombay, Powai, Mumbai 400 076, India

Received 14 July 2008; accepted 17 November 2008

DOI 10.1002/app.29698

Published online 17 April 2009 in Wiley InterScience (www.interscience.wiley.com).

ABSTRACT: PET-clay nanocomposites were prepared using alkyl quaternary ammonium and phosphonium modified clays by melt-mixing at 280°C using a micro twin screw extruder. The latter clays were prepared by synthesizing phosphonium surfactants using a simple one-step method followed by a cation exchange reaction. The onset temperature of decomposition (T_{onset}) for phosphonium clays (>300°C) was found to be significantly higher than that of ammonium clays (around 240°C). The clay modified with a lower concentration (0.8 meq) of phosphonium surfactant showed a higher T_{onset} as compared to the clay modified with a higher concentration (1.5 meq) of surfactants. Nanocomposites prepared with octadecyltriphenyl phosphonium (C18P) modified clay showed a higher extent of polymer intercalation as compared with benzyltriphenylphosphonium (BTP) and dodecyltriphenylphosphonium (C12P) modified clays. The nanocomposites prepared with ammonium clays showed a significant

decrease in the molecular weight of PET during processing due to thermal degradation of ammonium surfactants. This resulted in a substantial decrease in the mechanical properties. The molecular weight of PET was not considerably reduced during processing upon addition of phosphonium clay. The nanocomposites prepared using phosphonium clays showed an improvement in thermal properties as compared with ammonium clay-based nanocomposites. T_{onset} increased significantly in the phosphonium clay-based nanocomposites and was higher for nanocomposites which contained clay modified with lower amount of surfactant. The tensile strength decreased slightly; however, the modulus showed a significant improvement upon addition of phosphonium clays, as compared with PET. Elongation at break decreased sharply with clay. © 2009 Wiley Periodicals, Inc. *J Appl Polym Sci* 113: 1720–1732, 2009

Key words: clay; nanocomposites; polyesters

INTRODUCTION

Poly(ethylene terephthalate) (PET), a versatile thermoplastic polymer, is semicrystalline in nature with high mechanical strength and solvent resistance. This polymer is mainly used for making fibers, films and bottles.¹ Poly(ethylene terephthalate) is a condensation polymer and weakly polar in nature. It has high melting and processing temperatures. Further, it is prone to hydrolytic degradation in presence of small amounts of moisture. On account of its good mechanical properties, it has the potential for applications as an engineering plastic. Incorporation of nanoclays into PET provides an opportunity for further improvement in its mechanical, thermal and gas barrier properties.

Different methods of nanocomposite preparation are reported, viz., *in situ* polymerization, melt-intercalation and solvent intercalation.² Of these, melt-

intercalation or melt-mixing is a versatile method of nanocomposite preparation from an industrial point of view, as this method does not require an extra step or external agent (solvent) for nanocomposite preparation. Moreover, Vaia et al.³ have reported that nanocomposites (both intercalated and delaminated) can be synthesized by direct melt-intercalation even with high molecular weight polymers. Nevertheless, melt-mixing of high melting polymers with organoclays has certain disadvantages, for instance, molecular weight reduction in polymer because of low thermal stability of widely used ammonium modified clays.⁴ Hence, considerable research has been directed towards preparation of thermally stable organo-clays.^{4–6} Ammonium clays are reported to reduce the molecular weight of PET⁷ and of PA-6,⁸ during melt-mixing. Moreover, the hygroscopic nature of some polymers, for example, polyesters and polycarbonates has an adverse effect on the molecular weight during mixing with organoclays at high temperature.

Davis et al.⁷ prepared PET nanocomposites with two different organically modified clays via melt-blending at a processing temperature 285°C. Nanocomposites prepared with *N,N*-dimethyl-*N,N*-

Correspondence to: D. V. Khakhar (khakhar@iitb.ac.in).

Contract grant sponsor: University Grants Commission (UGC), India.

dioctadecylammonium treated montmorillonite, which has a decomposition temperature of 250°C, were black, brittle and tar-like resulting from degradation of the modifier under the processing conditions. However, nanocomposites prepared with 1,2-dimethyl-3*N*-hexadecyl imidazolium treated montmorillonite, which has a decomposition temperature of 350°C, showed a high level of dispersion and delamination. Mechanical and other properties were not reported in this study.⁷ Yoon et al.⁹ also found color formation in polycarbonate nanocomposites using different ammonium-based clays due to degradation of modifiers during melt processing at 260°C. Moreover, the presence of hydroxyl-ethyl group and unsaturated bonds in the alkyl chain of ammonium surfactant facilitated the molecular weight reduction in polycarbonate significantly.⁹ In another study, Fornes et al.¹⁰ observed the molecular weight degradation of nylon 6 during melt processing with ammonium-based clays. Again, they found that a higher level of clay exfoliation enhances polymer degradation due to exposure of surfactants to nylon 6 matrix. Saujanya et al.¹¹ studied the preparation of PET nanocomposites with expandable fluorine mica treated with 10-(3,5-bis(methoxycarbonyl)phenoxy)decyltriphenylphosphonium bromide by *in situ* polymerization process. At low contents of the clay, the melting, crystallization and glass transition temperature of PET increased. The effect of clay on mechanical properties was not reported.¹¹ Chang et al.¹² studied the preparation of PET-organoclay nanocomposites by *in situ* polymerization method followed by production of nanocomposite fibers by melt-spinning. In their study, dodecyltriphenyl phosphonium chloride was used as organic media to modify the clay. The tensile strength and modulus of the nanocomposite fibers increased from 46 to 71 MPa and from 2.2 to 4.1 GPa with 3 wt % of clay at a draw ratio of 1. The onset of degradation temperature was reported to be increased with clay loading up to 3 wt %.¹²

Ke et al.¹³ prepared PET nanocomposites with organically treated clay by intercalation of monomers followed by *in situ* polymerization. Details of organic modification were not mentioned in their study. They showed that with a 5 wt % clay loading, the tensile modulus of PET nanocomposites increased more than two times, and the heat distortion temperature was found to be 20–50°C higher than that of pure PET.¹³ In another study, an ion-exchanged clay modified with quaternary ammonium salt (Cloisite[®] 25A) was melt-mixed with recycled poly(ethylene terephthalate).¹⁴ The tensile modulus was reported to increase by 30% at 5 wt % clay loading. Tensile strength was found to be decreased slightly and strain at break decreased significantly.¹⁴ Suh et al.¹⁵ prepared unsaturated poly-

ester-montmorillonite nanocomposites using a two-step mixing method, in which, the unsaturated polyester was prepared using polyol from the glycolysis of PET and styrene monomer was used as a curing agent. They found that the two-step mixing method: mixing of polyester with montmorillonite clay and in the second step, mixing of styrene monomer with this blend was found to improve the level of dispersion of clay in the polymer matrix.¹⁵ Poly(ethylene terephthalate) ionomer-based clay nanocomposites were prepared by Barber et al.¹⁶ using two different organically modified clays (Cloisite 15A and Cloisite 10A). Nanocomposites were prepared by melt-blending in the temperature range of 240–255°C. Intercalated structures were obtained with pure PET. However, with sulfonated PET (ionomers), the clay layers were found to be exfoliated.¹⁶ Consequently, the tensile modulus increased significantly (about 38% at maximum) in these nanocomposites.¹⁶ Tensile strength of the nanocomposites was not reported.¹⁶

The present study focuses on the preparation and properties of PET-montmorillonite clay nanocomposites using various organically modified clays. Different phosphonium surfactants are synthesized by a simple one-step method, and montmorillonite clay is modified with two different amounts (0.8 and 1.5 meq) of phosphonium surfactants. PET nanocomposites are prepared using ammonium clays and the phosphonium clays via the melt-mixing method. The effect of different organoclays on the stability, and the thermal and mechanical properties of PET is studied.

EXPERIMENTAL

Materials

Cloisite Na⁺, unmodified clay and Cloisite 30B, a natural montmorillonite clay modified with methyl tallow bis-2-hydroxyethyl quaternary ammonium chloride were obtained from Southern Clay Products, USA. The cation exchange capacity (CEC) of Cloisite Na⁺ clay was found to be 95–100 meq/100 g of clay. PET granules, supplied by Reliance Industries, India, were of blow-molding grade, with $M_n \sim 39,000$. Triphenyl phosphine, benzyl chloride, 1-bromododecane and 1-bromooctadecane were used to synthesize the phosphonium surfactants. Petroleum ether was used to wash the synthesized product.

Synthesis of benzyltriphenylphosphonium chloride

The reaction was performed using a method similar to the one reported by Zhu et al.⁴ Figure 1 presents

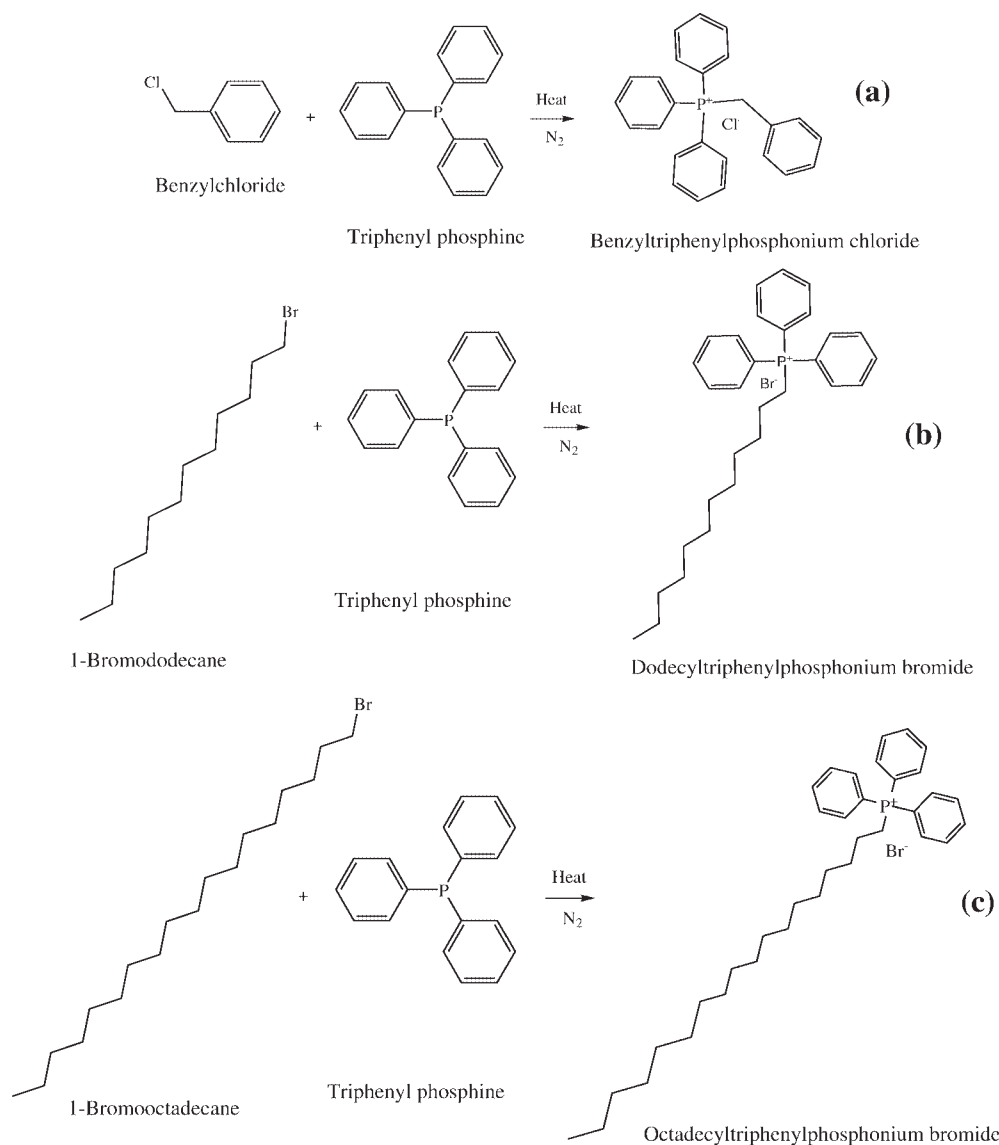


Figure 1 One-step synthesis method of phosphonium surfactants: (a) benzyltriphenylphosphonium chloride, (b) dodecyltriphenylphosphonium bromide, and (c) octadecyltriphenylphosphonium bromide.

a schematic view of the structure of the molecules and synthesis procedure. The required amounts of benzyl chloride (1.2M) and triphenylphosphine (1M) were placed in a 250 mL round bottomed flask. The reaction was performed at 100°C by stirring the reaction mixture with the help of a magnetic stirrer for 12 h. The final viscous product was washed thrice with petroleum ether. The yield was found to be about 80%. The product was dried for 12 h under vacuum at room temperature. ^{13}C and ^{31}P -NMR spectra were recorded on a VXR 300 NMR Spectrometer using CDCl_3 as solvent. The ^{13}C -NMR (CDCl_3 , δ , ppm) peaks were found to be at 134.6, 133.9 (d, $J = 9$ Hz, P-C coupling), 131.1 (d, $J = 5$ Hz, P-CH), 129.8 (d, $J = 12$ Hz, P-CH), 128.4, 128.0, 127.0 (d, $J = 8$ Hz, P-CH), 117.4 (d, $J = 84$ Hz, P-C), 30.2

(d, $J = 47$ Hz, P- CH_2) and the ^{31}P -NMR (CDCl_3 , δ , ppm) peak was found to be at 21.4, confirming the formation of the product.

Synthesis of dodecyltriphenylphosphonium bromide

The required amounts of triphenylphosphine (1M) and 1-bromododecane (1.2M) were placed in a 250 mL round bottomed flask. The reaction was performed at 100°C by stirring the reaction mixture with the help of a magnetic stirrer for 12 h. The final viscous product was washed three times with petroleum ether. The yield was found to be about 80%. The product was dried for 12 h under vacuum at room temperature. The ^{13}C -NMR (CDCl_3 , δ , ppm)

TABLE I
Nanocomposite Samples Prepared with Various Clays

Sample	Clay type	Modifier (y meq)	Clay percentage (x wt %)
PET	–	–	0
PET(x)CNa	CNa	–	3, 6, 9
PET(x)C30B	C30B	Methyltallow-bis-2-hydroxyethyl quaternary ammonium chloride	3, 5, 10
PET(x)BTP/y	BTP/y	Benzyltriphenyl phosphonium chloride	3, 6, 9
PET(x)C12P/y	C12P/y	Dodecyltriphenyl phosphonium bromide	3, 6, 9
PET(x)C18P/y	C18P/y	Octadecyltriphenyl phosphonium bromide	3, 6, 9

peaks were found to be at 134.9, 133.4 (d, $J = 10$ Hz, P-C), 130.3 (d, $J = 12$ Hz, P-C), 118.0 (d, $J = 85$ Hz, P-C), 31.6, 30.2 (d, $J = 15$ Hz, P-CH₂), 29.1 (m), 22.9, 22.4, 13.8, and the ³¹P-NMR (CDCl₃, δ , ppm) was at 22.1, confirming the formation of the product.

Synthesis of octadecyltriphenylphosphonium bromide

The required amounts of triphenylphosphine (1M) and 1-bromooctadecane (1.2M) were placed in a 250 mL round bottomed flask. The reaction was performed by stirring the mixture with a magnetic stirrer at 100°C for 10 h in nitrogen atmosphere. 1-Bromooctadecane was added slightly in excess to ensure the completion of the reaction. The product was washed three times with petroleum ether. The yield was found to be about 80%. The product was dried for 12 h under vacuum at room temperature. The product was dried for 12 h in vacuum at room temperature. The ¹³C-NMR (CDCl₃, δ , ppm) peaks were found to be at 135.0 (d, $J = 2$ Hz, P-C), 133.6 (d, $J = 10$ Hz, P-C), 130.5 (d, $J = 13$ Hz, P-C), 118.3 (d, $J = 85$ Hz, P-C), 31.8, 30.4 (d, $J = 15$ Hz, P-CH₂), 29.3 (m), 23.1, 22.6, 14.0, and the ³¹P-NMR (CDCl₃, δ , ppm) was at 22.4, confirming the formation of the product.

Clay modification using phosphonium surfactants

The clay was modified using 0.8 and 1.5 meq of the surfactants by cation exchange reaction. An unmodified clay (Cloisite Na⁺) (10 g) was dispersed in 500 mL of deionized water using a magnetic stirrer at 60°C. Different amounts of the surfactants (determined using cation exchange capacity) were dissolved in a 50 : 50 mixture of water and methanol. The solution was slowly transferred into the clay suspension along with stirring. A white precipitate was observed immediately after the transfer of the surfactant solution, indicating the beginning of exchange reaction. The reaction was continued for 12 h to ensure the complete exchange of cations. The suspension was filtered and washed repeatedly with mixture of water and methanol until the white pre-

cipitate of the chloride ion with AgNO₃ solution was not obtained. The clay was vacuum-dried for 24 h at 100°C. The lumps of clay after drying were ball-milled into a fine powder of initial size.

Nanocomposite preparation and characterization

PET-clay nanocomposites were prepared by the melt-mixing method in a twin-screw micro-compounder (DSM) having a corotating double-screw and a capacity of 5 g per batch. Before mixing, the materials were dried in a vacuum oven at 130°C for 12 h. Various amounts of clays were melt-mixed with the polymer. The processing temperature, residence time of mixing and screw speed were set at 280°C, 6 min and 150 rpm, respectively. Several batches of samples were prepared for various studies. The acronyms for the different samples are given in Table I.

Solution viscosity measurements

The samples were dissolved in a mixture of phenol and 1,1,2,2-tetrachloroethane (60 : 40 by volume). The relative viscosity (η_{rel}) defined as the ratio of the solution viscosity to solvent viscosity was measured using a Ubbelohde capillary viscometer at 25°C. The intrinsic viscosity was determined from a single point measurement of η_{rel} , using the following approximation for linear polymers¹⁷

$$[\eta] = \sqrt{2/C} \sqrt{\eta_{sp} - \ln \eta_{rel}} \quad (1)$$

The number average molecular weight, M_n , was determined from the Mark-Houwink relation, $[\eta] = KM_n^\alpha$, where $K = 7.44 \times 10^{-4}$ dL g⁻¹ and $\alpha = 0.648$ at 25°C.¹⁸

Wide angle x-ray diffraction

WAXD studies were performed for all the samples using Cu-K α radiation of wavelength 1.54 Å. between 3 and 12° 2 θ at 0.02°/20s using a x-ray diffractometer (X'Pert Pro, PANalytical).

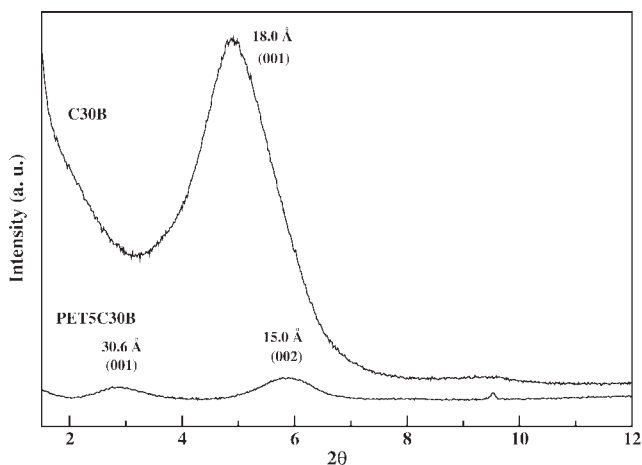


Figure 2 Wide angle x-ray diffraction patterns of ammonium modified clay and PET-clay nanocomposites. The shifting of (001) plane peak towards left or increase in d -spacing indicates intercalation of polymer chains into clay galleries.

Small angle x-ray scattering

SAXS experiments were performed on thick polymer films cut from tensile samples of thickness around 1 mm using an x-ray source of wavelength 1.54 Å in a diffractometer (Anton Paar, Austria). The samples were scanned between $2\theta = 0.058$ – 11.0° at 25°C for 15 min. The scattering patterns were recorded on a film using line collimation technique. The scattering patterns were integrated to generate an $I(q)$ versus q curve, where $I(q)$ is the intensity of scattered x-rays and q is the scattering vector.

Transmission electron microscopy

TEM (Philips CM 200) was performed to study the dispersion of clay. Samples for TEM were prepared using ultra-microtome (Leica, Ultracut UCT). Around 70–100 nm thick films were cut along the flow direction of injection-molded tensile specimen using a freshly prepared glass knife. The thickness of the films was determined from the given color chart. One of the films was transferred to a 200 mesh carbon coated copper grid and stained with osmium tetroxide for about half an hour before analysis.

Dynamic mechanical analysis

Dynamic mechanical analysis was performed in the cantilever bending mode on bar-like samples cut from tensile samples of width, thickness and length 4.7 (± 0.1) mm, 1.4 (± 0.1) mm, and 10.2 (± 0.3) mm, respectively, in a dynamic mechanical analyzer (Triton, UK). Experiments were performed between room temperature and 200°C at the heating rate of $4^\circ\text{C}/\text{min}$. The frequency of bending and deflec-

tion (strain) were fixed at 1 Hz and 0.02 mm, respectively.

Thermogravimetric analysis

Thermogravimetric analysis (High resolution TGA 2950, TA instruments) studies were performed in N_2 atmosphere between room temperature and 800°C at the rate of 20°C per min.

Tensile measurements

The samples were injection-molded in a micro injection-molding machine (DSM, Holland) from melt at 280°C to make tensile specimens. The mold was kept at 70°C . Tensile testing was conducted on the dumb-bell shaped specimens (ASTM D638 Type V) using a universal testing machine (Hounsfield UTM) equipped with a 10 kN load cell. The cross-head speed was set at 5 mm/min.

RESULTS AND DISCUSSION

Nanocomposites using ammonium-based clay

Figure 2 shows the wide angle x-ray diffraction patterns for C30B and PET-clay nanocomposites with 5 wt % of C30B. The (001) plane for C30B is seen at $2\theta = 4.9^\circ$, corresponding to a d -spacing of 18.0 Å. However, in nanocomposites the peak is shifted to $2\theta = 2.9^\circ$, corresponding to a d -spacing of 30.6 Å, indicating formation of intercalated nanocomposites. Another peak at $2\theta = 5.9^\circ$ is observed in the nanocomposites, which is a peak for (002) plane with a corresponding d -spacing of 15.0 Å.¹⁶

The intrinsic viscosity ($[\eta]$) and average molecular weight (M_n) of PET are listed in Table II. The intrinsic viscosity and weight average molecular weight of as-received PET are found to be 0.70 dL g^{-1} and $38,795 \text{ g mol}^{-1}$, respectively. After processing of PET at 280°C , $[\eta]$ decreases slightly, indicating a 19% decrease in M_n . However, the reduction in molecular weight is significant with 10 wt % C30B (Table II). This is due to degradation of ammonium modifier

TABLE II
Intrinsic Viscosity $[\eta]$, and Average Molecular Weight of PET and PET After Processing (PET/AP) and PET-Clay Nanocomposites

Samples	$[\eta]$ (dL g^{-1})	M_n (g mol^{-1})
PET	0.70	38,795
PET/AP	0.61	31,372
PET3C30B	0.42	17,637
PET5C30B	0.40	16,357
PET10C30B	0.36	14,142
PET6CNa	0.49	22,092

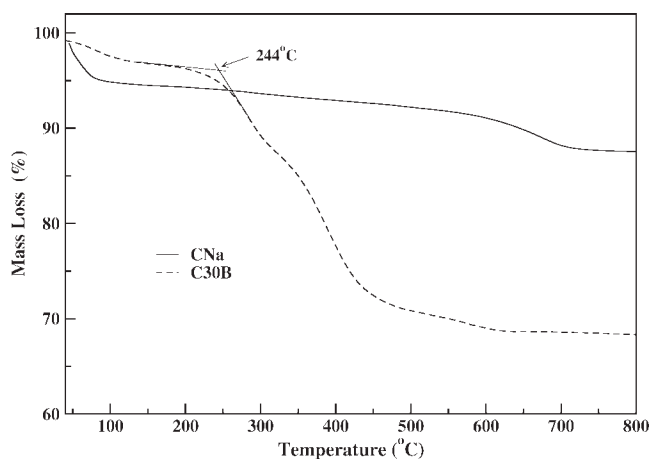


Figure 3 Thermogravimetric analysis of unmodified clay (CNa) and ammonium modified clay (C30B).

during processing, as the onset of decomposition temperature for ammonium clay ($\sim 245^\circ\text{C}$), shown in TGA curves for unmodified clay (CNa) and C30B (Fig. 3), is lower than processing temperature (280°C) of PET. PET with 5% unmodified clay also showed a decrease in molecular weight, however, the reduction was much less than that for organo-clay composites.

The dynamic storage modulus versus temperature curves for PET and PET-clay nanocomposites are plotted in Figure 4. The storage modulus increases significantly for composites with clay throughout the temperature range. The storage modulus of PET nanocomposites having 5 and 10 wt % organo-clay (C30B) increases reasonably by 21 and 22%, respectively, at 30°C . The composites with 5% of unmodified clay (CNa) also show a slight increase in storage modulus at 30°C . At higher temperatures, the storage modulus further increases with clay con-

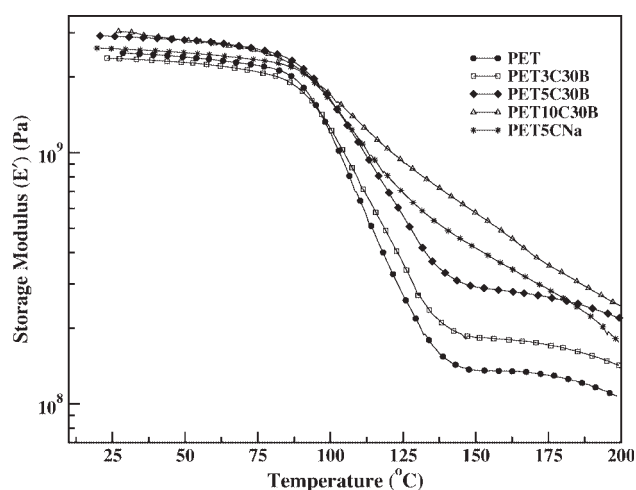


Figure 4 Storage modulus versus temperature curves of PET-clay nanocomposites, storage modulus increases with both the ammonium and unmodified clay.

TABLE III
Mechanical Properties of PET-Clay Nanocomposites, Clay Modified with Quaternary Ammoniums

Sample	Tensile strength (MPa)	Elongation at break (%)
PET	52.4	244
PET3C30B	39.2	10
PET5C30B	39.6	9
PET10C30B	14.9	9

tent. The storage modulus for 10 wt % C30B at 150°C increases significantly (four times that of PET). At higher temperatures, the storage modulus for 5 wt % of CNa is higher than that of with 5 wt % C30B. This may be because the molecular weight in the former case is higher than that in the latter case (Table II). For 5 wt % of C30B nanocomposites, the storage modulus is two times that of PET.

The tensile strength and modulus values are given in Table III. The nanocomposites containing 10 wt % organo-clay (C30B) show a decrease in tensile strength and modulus. At this clay percentage, the material is poor in quality and brittle in nature. However, the hybrid materials with 3 and 5 wt % of organo-clay show 18 and 22% increase in tensile modulus, respectively. Tensile strength decreased with 3 and 5 wt % of C30B compared with PET, whereas with 5 wt % CNa, the strength is nearly the same as pure PET but the tensile modulus is higher. The significant reduction in molecular weight in ammonium clay-based nanocomposites results in significant degradation of tensile strength (Table III). However, the properties improve slightly with unmodified clay. This indicates that the thermal stability of the organic surfactant present in clay is important in the final properties of PET nanocomposites as reported earlier.^{9,19}

Characterization of phosphonium clays

Figures 5 and 6 show x-ray diffraction patterns of unmodified and the phosphonium modified clays. The WAXD patterns for clay modified with 0.8 meq of phosphonium surfactants are given in Figure 5, whereas that of clay modified with 1.5 meq of phosphonium surfactants are given in Figure 6. The unmodified clay has a $d_{(001)}$ -spacing of 12.3 \AA , the XRD peak for which is seen at $2\theta = 7^\circ$. The d -spacing value is slightly higher than the actual d -spacing of unmodified clay (9.6 \AA) in perfectly dried condition. This indicates hygroscopic nature of the montmorillonite clay. Modification of clay with the phosphonium surfactants results in a shift in the (001) peak by 2.5° , in all the cases. This corresponds to an increase in d -spacing of about 6 \AA , indicating that the surfactant molecules are intercalated into

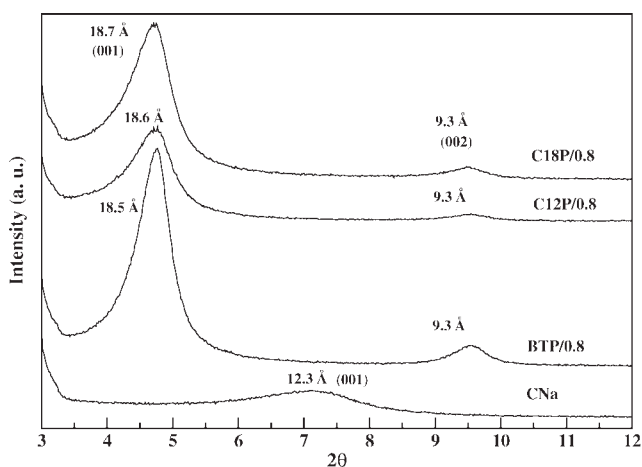


Figure 5 Wide angle x-ray diffraction patterns of unmodified and clay modified with 0.8 meq of different phosphonium surfactants, showing the d -spacing of the clays.

the clay galleries. Further, a new peak appears at $2\theta = 9.5^\circ$, which corresponds to a d -spacing of 9.3 Å and is a (002) diffraction plane of clay.¹⁶ This peak position remains constant in all the phosphonium clays. Clays modified with 1.5 meq surfactants show a higher $d_{(001)}$ -spacing than the modified with 0.8 meq surfactants. This indicates that more number of surfactant molecules reside in the interlayer gallery of clay. As expected, C18P/1.5 (Fig. 6), which contains a C18 carbon chain in its backbone, shows a $d_{(001)}$ -spacing of 19.5 Å, which is higher than the clays modified with other surfactants with same concentration. Similarly, C18P/0.8 (Fig. 5) shows a slightly higher $d_{(001)}$ -spacing (18.7 Å) than C12P/0.8 (18.6 Å) and BTP/0.5 (18.5 Å). BTP/1.5 shows a higher $d_{(001)}$ -spacing than C12P/1.5.

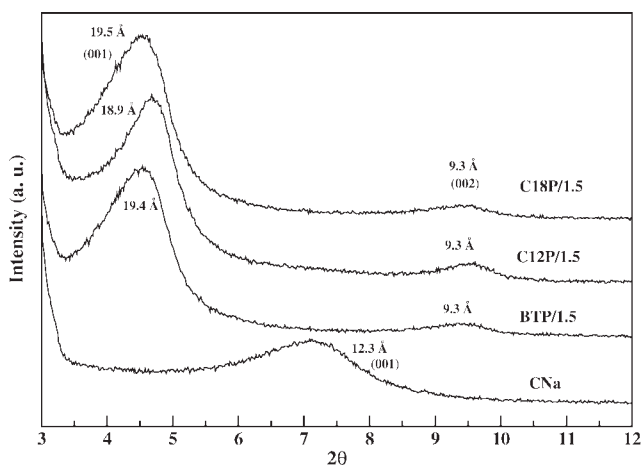


Figure 6 Wide angle x-ray diffraction patterns of unmodified and clay modified with 1.5 meq of different phosphonium surfactants showing the d -spacing of the clays.

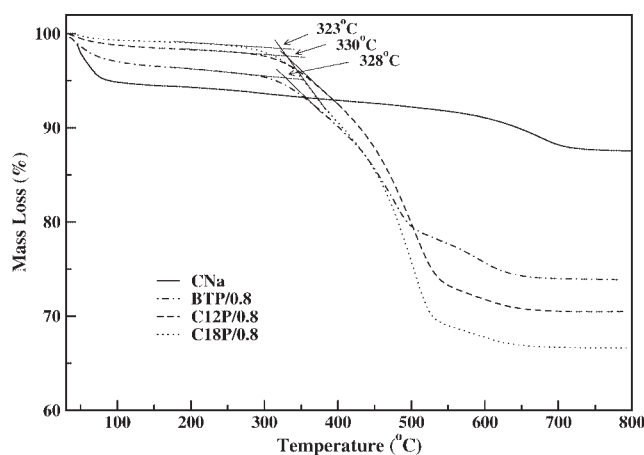


Figure 7 Thermogravimetric analysis of unmodified and clay modified with 0.8 meq of different phosphonium surfactants. The onset of degradation temperature was determined by drawing tangents.

The percentage mass loss with temperature curves for unmodified and clays modified with different amount of phosphonium surfactants are plotted in Figures 7 and 8. The unmodified clay does not show a significant mass loss up to 600°C. The initial mass loss below 200°C is due to evaporation of free water in the clay. The mass loss between 500 and 800°C is due to evaporation of structural water which undergoes dehydroxylation.²⁰ However, in the case of organoclays, the major mass loss happens in the temperature range of 200–500°C.²¹ The onset of decomposition temperature (T_{onset}) for C30B is found to be 244°C as quaternary ammonium ions start degrading from this temperature onwards (Fig. 8). However, the T_{onset} increased significantly (59–86°C higher than C30B) for phosphonium surfactant

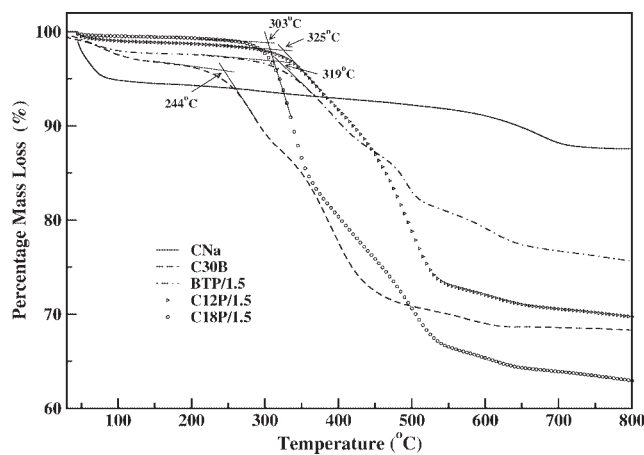


Figure 8 Thermogravimetric analysis of unmodified, ammonium and clay modified with 1.5 meq of different phosphonium surfactants, showing the onset of degradation temperature.

TABLE IV
Onset of Degradation and Mass Loss of Unmodified, Ammonium Modified, and Phosphonium Modified Clays, Determined from Thermo-Gravimetric Analysis

Sample	T_{onset} ($^{\circ}\text{C}$)	Total mass loss (%)	Organic content (%)
CNa	595	12.4	0
C30B	244	31.5	27.0
BTP/0.8	328	26.1	19.2
C12P/0.8	330	29.4	25.8
C18P/0.8	323	33.3	30.6
BTP/1.5	319	29.5	19.0
C12P/1.5	325	30.3	26.0
C18P/1.5	303	36.9	33.5

modified clays as shown in Figures 7 and 8. The T_{onset} and percentage mass loss values for different clays, determined from TGA curves, are listed in Table IV. The T_{onset} is found to be lower for the higher surfactant concentration. Clays modified with 0.8 meq of phosphonium surfactant showed around 5–20 $^{\circ}\text{C}$ higher T_{onset} than that of with 1.5 meq of phosphonium surfactant. This may be due to degradation of weakly bonded excess surfactant molecules present in the intergallery spacing of clay. The TGA curves (Figs. 7 and 8) also reveal that the phosphonium clays modified with 1.5 meq of phosphonium surfactants show higher percentage of mass loss between 200 and 500 $^{\circ}\text{C}$ compared with those modified with 0.8 meq of surfactant (Table IV). It can be observed that the percentage mass loss sharply increases for C18P/1.5 (Fig. 8), indicating degradation of long chain alkyl molecules. C12P shows higher T_{onset} for both concentrations of surfactants as compared with other phosphonium clays, whereas C18P shows the lowest T_{onset} . The highest $T_{\text{onset}} = 330^{\circ}\text{C}$ is obtained for C12P/0.8 which is 86 $^{\circ}\text{C}$ higher than that of ammonium clay. C18P/1.5 shows the highest percentage of mass loss (36.9%). It also contains the highest amount of organic content (33.5%). This is mainly because the C18P modifier has the highest molecular weight of the phosphonium surfactants used. The initial mass loss between room temperature to T_{onset} which is mainly due to evaporation of moisture, is lower for C18P/0.8 (1.5%) (Fig. 7) and C18P/1.5 (1.2%) (Fig. 8) than that for other clays. This indicates that the clay modified with larger alkyl chain (C18P) is more hydrophobic and absorbs less moisture.

Figure 9 presents the TGA and DTG of C18P surfactant and clay modified with the surfactant. From the mass loss versus temperature curves [Fig. 9(a)], it is clear that T_{onset} for C18P clay (323 $^{\circ}\text{C}$) is significantly higher than that for C18P surfactant (270 $^{\circ}\text{C}$). This indicates that the surfactant molecules are adsorbed or bonded onto the clay surface and higher energy is needed to dissociate the surfactant mole-

cules from clay surface followed by decomposition. The derivative mass versus temperature curves for the surfactant and clay modified with the surfactant are given in Figure 9(b). It can be seen that the decomposition of surfactant is a one-step process and the maximum rate of mass loss (peak) is seen at 310 $^{\circ}\text{C}$. However, the organoclay degrades in two steps and the peaks are observed at 340 and 465 $^{\circ}\text{C}$. This indicates that the ionically bonded surfactants with clay are more thermally stable than the surfactants in its pure form. This is in agreement with the recent work of Cui et al.,²² who performed a detailed study of the thermal degradation of ammonium surfactants and organoclays based on the surfactants. The peak height for the second event is higher than the first. So, the maximum amount of mass loss occurs at the higher temperature. The initial degradation of clay or the first peak could be due to the Hoffmann-type elimination reaction in phosphonium salts²³ in presence of hydroxyl groups of clay which causes the detachment of surfactants from clay surface. The second degradation or the second peak is due to the degradation of the byproducts of the above reaction.

Nanocomposites using phosphonium-based clays

The d -spacings of the different clays and of the clays dispersed in PET, obtained from WAXD and SAXS, are summarized in Table V. The $d_{(001)}$ spacing for each sample is roughly double of the $d_{(002)}$ spacing, as required, and thus a combination of these two

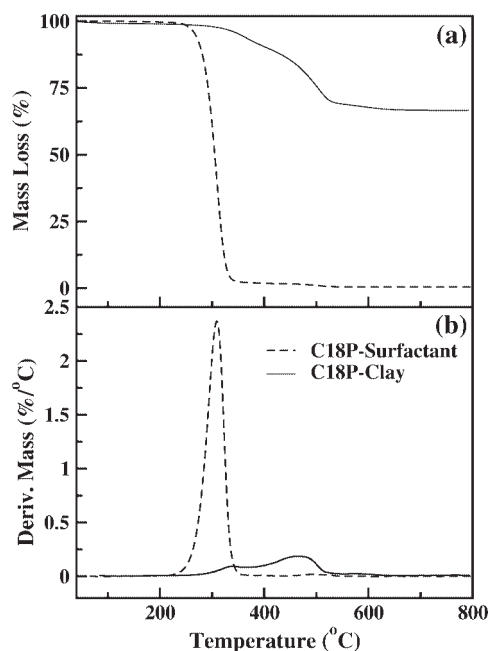


Figure 9 Thermogravimetric analysis of C18P surfactant and C18P clay (a) mass loss versus temperature, (b) derivative mass versus temperature curves.

TABLE V
The d -Spacing Corresponding to Different Planes of Clays and Clay Peak in Nanocomposites Determined from WAXD and SAXS

Clay type	$d_{(001)}$ -Spacing (Å)				$d_{(002)}$ -Spacing (Å)			
	Pure clay	Clay amount in nanocomposites (wt %)			Pure clay	Clay amount in nanocomposites (wt %)		
		3	6	9		3	6	9
CNa	12.3	16.2	15.9	15.2				
BTP/0.8	18.5	20.9	21.5	21.7	9.3	9.9	10.1	10.1
C12P/0.8	18.6	19.3	19.7	20.0	9.3		9.7	9.7
C18P/0.8	18.7	35.9 ^a	34.5 ^a		9.3	19.4	18.9	18.7
BTP/1.5	19.4		20.9		9.3		9.8	
C12P/1.5	18.9	18.9	18.8	19.1	9.3		9.4	9.4
C18P/1.5	19.5		38.5 ^a		9.3	18.8	19.3	

^a d -spacing, determined from SAXS analysis.

data sets for $d_{(001)}$ and $d_{(002)}$ gives a reasonable description of the characteristics of the layered structures in the nanocomposites. We note that the existence of peaks in the X-Ray diffraction traces only implies the existence of layered structures but does not give complete information about the dispersion of clay in the nanocomposite. This is because layered aggregates may coexist with exfoliated clay layers. With this caveat, we make the following inferences from the data in Table V. The polymer intercalates only to a small extent in the unmodified clay (CNa), but to a significantly larger extent in the organically modified clays as evidenced by the larger d -spacings obtained in the latter. The amount of intercalation increases with length of the alkyl chain of the surfactant (the d -spacing for C18P is greater than that for C12P) and with increase in surfactant loading (the d -

spacing is slightly higher for 1.5 meq of surfactant as compared with 0.8 meq). These results are physically reasonable considering that the surfactant results in a hydrophobic environment in the clay galleries.

Figure 10 shows the bright field TEM images of PET-clay nanocomposites. The osmium tetroxide stains the clay and the dark areas represent clay phase in polymer matrix. As the thin sections are cut from injection molded specimens, it can be clearly observed that the clay layers align in the direction of flow. PET with 6 wt % C18P/0.8 shows uniform clay dispersion in polymer matrix [Fig. 10(a)]. This is in good agreement with small angle x-ray scattering analysis, which shows the highest degree clay intercalation from d -spacing of 18.7 Å for C18P/0.8 to 34.5 Å in the nanocomposites.

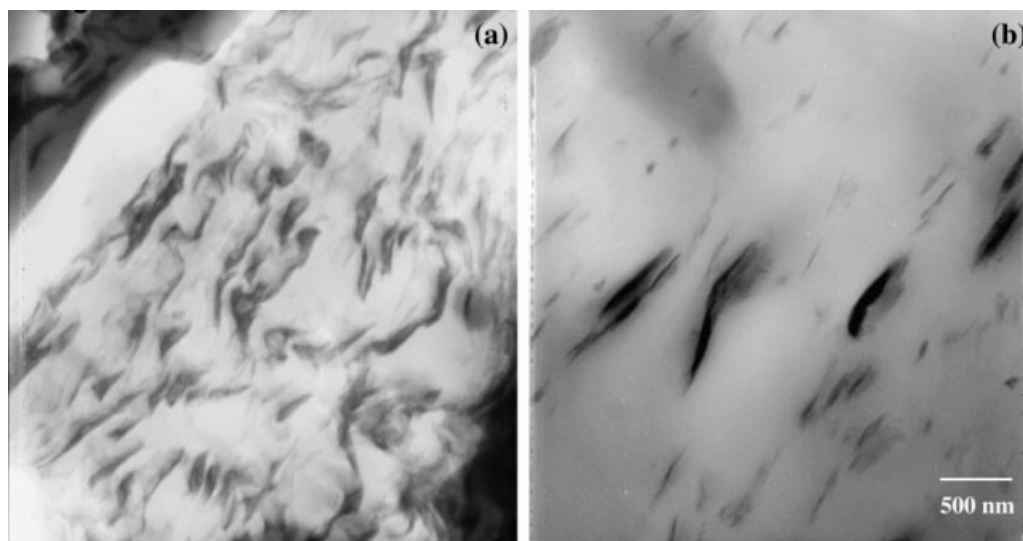


Figure 10 Bright field transmission electron microscopy images of PET-phosphonium modified clay nanocomposites. (a) PET with C18P/0.8 (PET6C18P/0.8) showing a good dispersion of clay layers and (b) PET with C12P/0.8 (PET6C12P/0.8), showing a slight aggregation of clay layers, however, some of the clay layers are exfoliated. Both the images are at same magnifications.

TABLE VI
Intrinsic Viscosity $[\eta]$ and Average Molecular Weight of PET, PET After Processing (PET/AP), and PET-Clay Nanocomposites with Phosphonium Clays

Samples	$[\eta]$ (dL g ⁻¹)	M_n (g mol ⁻¹)	T_{onset} (°C)
PET	0.70	38,795	—
PET/AP	0.58	28,784	399
PET3CNa	—	—	410
PET6CNa	0.49	22,092	413
PET3BTP/1.5	0.46	20,288	—
PET6BTP/1.5	0.42	17,397	410
PET9BTP/1.5	0.49	22,303	—
PET3C18P/1.5	0.48	21,952	411
PET6C18P/1.5	0.45	19,820	412
PET9C18P/1.5	0.45	19,430	415
PET3BTP/0.8	0.56	27,796	—
PET6BTP/0.8	0.55	26,739	421
PET9BTP/0.8	0.51	23,654	420
PET3C12P/0.8	0.58	29,317	420
PET6C12P/0.8	0.55	26,882	422
PET9C12P/0.8	0.53	24,872	421
PET3C18P/0.8	0.53	24,989	422
PET6C18P/0.8	0.50	22,918	421
PET9C18P/0.8	0.50	22,726	427

At this d -spacing of clay in nanocomposites, the clay is suggested to be exfoliated.²⁴ TEM of PET-clay nanocomposites with C12P is given in Figure 10(b). Although a good dispersion of clay is obtained, but there are still some aggregated clay layers present in this nanocomposites. The number of clay tactoids per unit area in C12P nanocomposites is small as compared with C18P nanocomposites (Fig. 10), indicating a good dispersion in the latter case.

Table VI presents the intrinsic viscosity and average molecular weight for PET and PET nanocomposites with phosphonium clays. The M_n is reduced slightly and is found to be about 28,784 g mol⁻¹

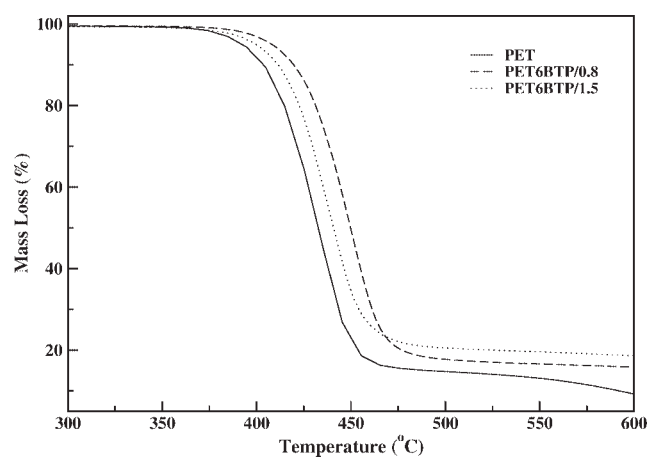


Figure 11 Thermogravimetric analysis curves of PET and PET-clay nanocomposites with BTP clay modified with two different concentrations of phosphonium showing the onset of decomposition temperature (T_{onset}) is higher for lower concentration of clay modifier.

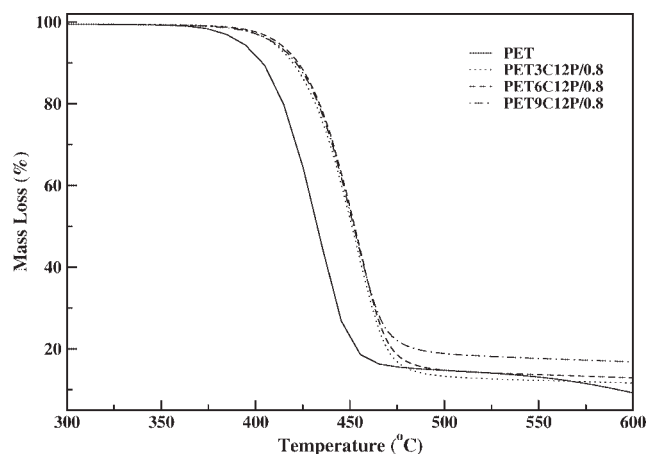


Figure 12 Thermogravimetric analysis curves of PET and PET-clay nanocomposites with C12P/0.8 clay showing an increase in onset of decomposition temperature (T_{onset}) with clay.

when PET is processed at 280°C for 6 min. The processing is performed to have a comparison with M_n of nanocomposite samples, which are also melt-mixed for the same time period. This may be due to thermal degradation or hydrolytic degradation of PET in presence of moisture during processing. The IV decreased compared to as-received PET beads upon addition of phosphonium clay. However, the values are comparable to IV of PET/AP (PET after processing). Addition of phosphonium clay with 1.5 meq of modifier shows a greater decrease in the M_n than that with 0.8 meq of modifier concentration in clay. This indicates that higher amount of organic modifier in clay can adversely affect on the molecular weight of PET. This may be due to the excessive amount of modifier which adsorbed onto the clay surface starts degrading at the processing conditions, which causes the molecular weight reduction. The nanocomposites with 3 wt % C12P/0.8 (PET3C12P/

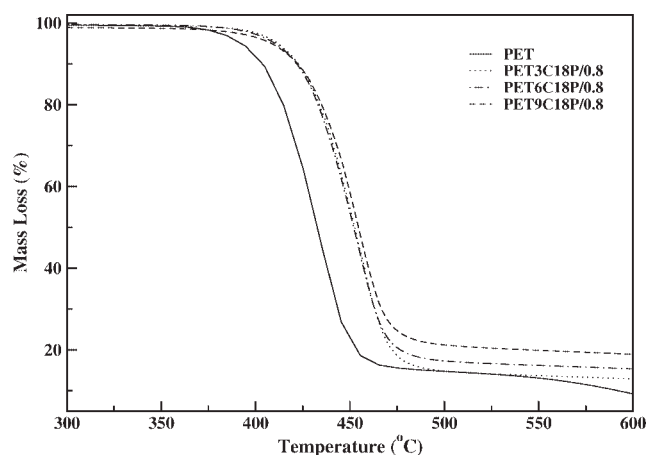


Figure 13 Thermogravimetric analysis of PET and PET-clay nanocomposites with C18P/0.8 showing an increase in T_{onset} with clay.

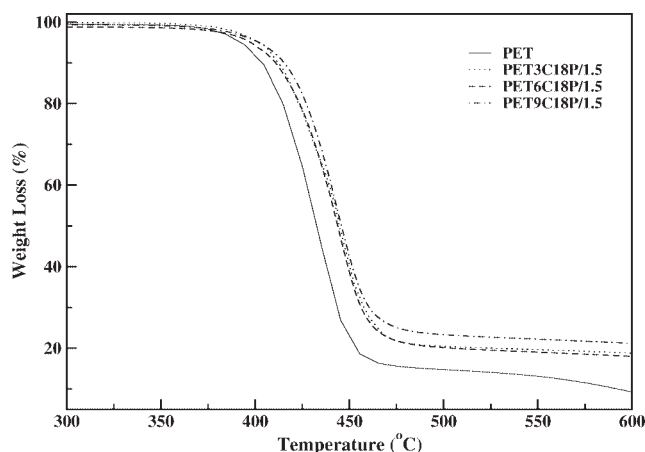


Figure 14 Thermogravimetric analysis of PET and PET-clay nanocomposites with C18P/1.5 showing an increase in T_{onset} with clay.

0.8) are found to be the best composite in terms of molecular weight retention.

Figure 11 presents the thermogravimetric analysis curves of PET and PET-clay nanocomposites with BTP clay. The onset temperature of decomposition (T_{onset}) increases significantly with BTP. PET shows a T_{onset} of 399°C, whereas the nanocomposites show around 10–20°C higher in the T_{onset} . The T_{onset} values for different nanocomposite samples are listed in Table IV. Nanocomposites prepared with clay having lower concentration (0.8 meq) of modifier show around 10°C higher T_{onset} than with higher concentration (1.5 meq) of modifier (Fig. 12). This may be related to the higher degree of intercalation in nanocomposites with lower concentration of clay modifier than that of with higher concentration of clay modifier.

Figure 12 presents the TGA curves of PET and PET-clay nanocomposites with C12P/0.8. The T_{onset}

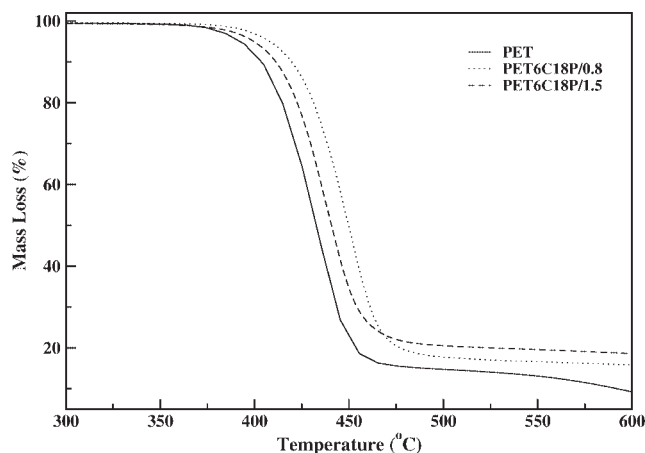


Figure 15 Thermogravimetric analysis of PET and PET-clay nanocomposites with C18P/1.5 and C18P/0.8 showing T_{onset} is higher for C18P/0.8 than C18P/1.5.

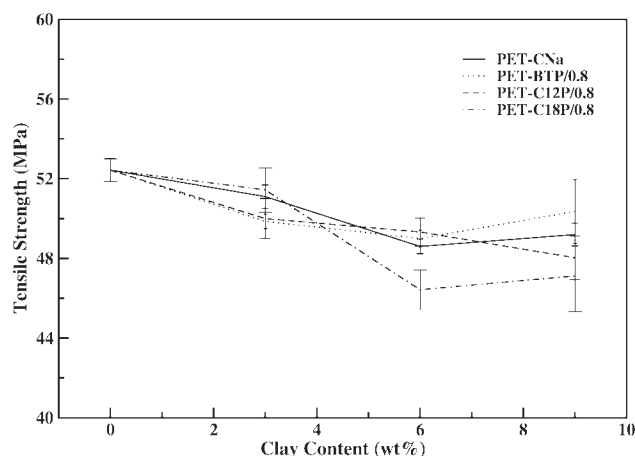


Figure 16 Tensile strength of PET-clay nanocomposites with clay modified with 0.8 meq of phosphonium surfactant.

increases by around 20°C with C12P/0.8 for all the concentrations of clay (Fig. 13). The T_{onset} values for different samples are presented in Table VI. TGA curves of PET and PET-clay nanocomposites using C18P clay with different concentrations (0.8 and 1.5 meq) of modifier are presented in Figures 13–15. The nanocomposites prepared with C18P/0.8 show around 23–28°C increase in T_{onset} (Fig. 13), whereas nanocomposites with C18P/1.5 show a relatively smaller increase (around 10–15°C) in the T_{onset} (Fig. 13) compared with the T_{onset} of PET. Figure 15 shows a comparison between two different modifier concentrations in clay. PET9C18P/0.8 shows the highest T_{onset} (427°C) as compared with all other nanocomposites (Fig. 13).

The tensile properties of PET and PET-clay nanocomposites are shown in Figures 16–18. The clays used are modified with 0.8 meq of phosphonium surfactants. The tensile strength for pure PET is

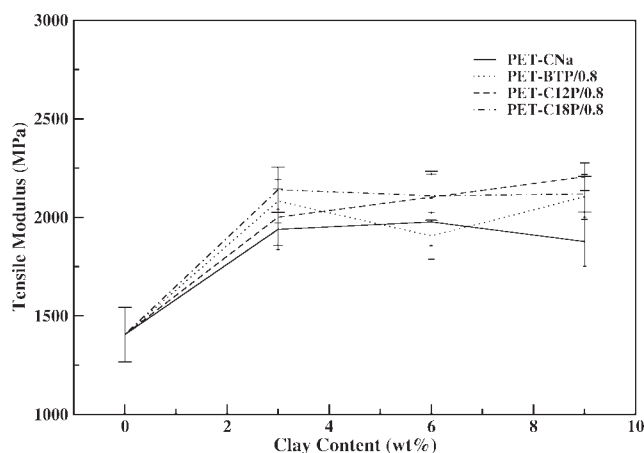


Figure 17 Tensile modulus of PET-clay nanocomposites with clay modified with 0.8 meq of phosphonium surfactant.

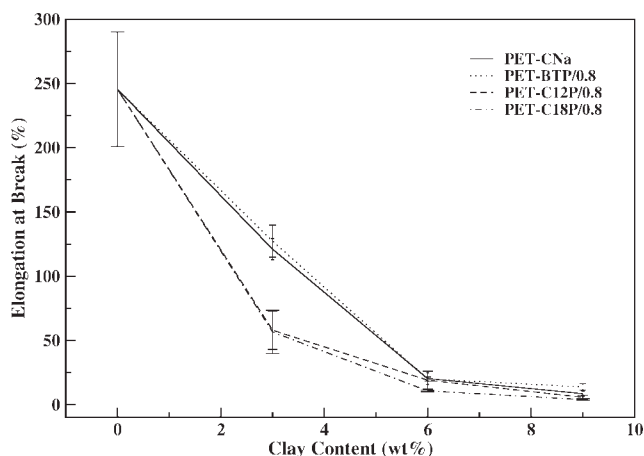


Figure 18 Elongation at break of PET-clay nanocomposites with clay modified with 0.8 meq of phosphonium surfactant.

found to be 52.4 MPa. The strength slightly decreases upon addition of all the clays. The strength is not affected much with BTP/0.8 and C12P/0.8; however, it decreases slightly higher with 6 and 9 wt % of C18P/0.8 (Fig. 16). This may be due to their low molecular weight as compared to nanocomposites with other organoclays (Table VI). The tensile modulus increases significantly (around 36–57%) with addition of phosphonium clay (Fig. 17). The maximum increase in modulus (57%) is observed with 9 wt % of C12P/0.8. Addition of unmodified clay (CNa) also increases the tensile modulus. However, the increase (around 35–40%) is lesser than that for phosphonium clays. The reason may be a better interaction of polymer chains with phosphonium modified clay than with unmodified clay. Elongation at break decreases significantly with small amount of clay (Fig. 18). PET showed around 250% elongation at break. However, it decreased to a minimum of 4% with 9 wt % of C18P/0.8. Nanocomposites with a lower amount of phosphonium clays showed a significant increase in modulus and better retention of strength and elongation. Particularly, nanocomposites with 3 wt % BTP/0.8 gave the best balance of mechanical properties in terms of modulus and elongation at break.

CONCLUSIONS

Phosphonium surfactants were synthesized to prepare thermally stable organoclays. Phosphonium surfactant-based montmorillonite clays were found to have onset of decomposition temperatures around 50–80°C higher than those for ammonium modified clays (around 240°C). The onset of decomposition temperature was found to be higher for the clays having a lower concentration of phosphonium surfactant. Dodecyltriphenylphosphonium bromide (C12P)

modified clay showed the highest onset of decomposition temperature (330°C) with 0.8 meq of surfactant. Higher concentration (1.5 meq) of phosphonium surfactants in clay showed higher $d_{(001)}$ -spacing than that of lower surfactant concentration (0.8 meq). The clay modified with 1.5 meq of phosphonium surfactants showed the highest mass loss between 200 and 500°C compared with that modified with 0.8 meq of surfactants.

Poly(ethylene terephthalate)-clay nanocomposites were prepared using unmodified, ammonium and phosphonium modified clays by melt-mixing at 280°C. It was found that the molecular weight of PET, obtained from intrinsic viscosity measurements, decreased significantly in nanocomposites while processing with ammonium modified clay. The resulting nanocomposites showed a significant decrease in tensile strength with ammonium clay. However, the storage modulus increased with ammonium clay. The nanocomposites prepared with unmodified clay showed formation of intercalated nanocomposites. The nanocomposites prepared with phosphonium clays with different surfactant loadings showed different extents of intercalation as inferred from the measured d -spacing. Octadecyltriphenylphosphonium (C18P) modified clay showed the highest degree of intercalation or exfoliation of clay layers among the clays used. The nanocomposites prepared with a higher surfactant concentration (1.5 meq) in C18P showed a greater polymer intercalation compared to that with lower surfactant concentration (0.8 meq). However, in the case of benzyltriphenylphosphonium (BTP) and dodecyltriphenylphosphonium (C12P) modified clays, the nanocomposites prepared with a higher surfactant concentration (1.5 meq) in clay showed a smaller degree of polymer intercalation than that with a lower surfactant concentration (0.8 meq). Molecular weight decreased only slightly during processing in nanocomposites prepared with unmodified clay and phosphonium clays. The nanocomposites with higher concentration of clay modifier showed greater decrease in molecular weight as compared to that with lower concentration of modifier.

The onset temperature of decomposition of the nanocomposites increased significantly (10–28°C) with phosphonium clay. Again, the onset temperature of decomposition of nanocomposites was higher for clay with lower concentration of surfactants in all the clays. Tensile strength of nanocomposites remained unaltered or decreased slightly. However, the tensile modulus values increased significantly. Nanocomposites based on phosphonium clays showed higher modulus than those with unmodified clay. The maximum increase in tensile modulus (57%) was observed for dodecyltriphenylphosphonium clay (C12P/0.8). The elongation at break

decreased sharply with clay addition, and the lowest elongation at break (4%) was obtained for 9 wt % of C18P/0.8. The elongation at break decreased with increasing clay loading. Nanocomposites with 3 wt % BTP/0.8 gave the best balance of mechanical properties in terms of modulus and elongation at break.

The SAIF, IITB is acknowledged for providing TEM facilities. Mr. Sangram Rath, NMRL, Ambarnath are acknowledged for TGA experiments.

References

1. Billmeyer, F. W. J. Text Book of Polymer Science, 3rd ed.; Wiley: New York, 1984.
2. Alexandre, M.; Dubois, P. Mater Sci Eng R Rep 2000, 28, 1.
3. Vaia, R. A.; Ishii, H.; Giannelis, E. P. Chem Mater 1993, 5, 1694.
4. Zhu, J.; Morgan, A. B.; Lamelas, F.; Wilkie, C. Chem Mater 2001, 13, 3774.
5. Gilman, J.; Awad, W.; David, R.; Shields, J.; Harris, R. H.; Morgan, A.; Sutto, T.; Callahan, J.; Trulove, P. C.; DeLong, H. Chem Mater 2002, 14, 3776.
6. Zhu, J.; Uhl, F. M.; Morgan, A. B.; Wilkie, C. A. Chem Mater 2001, 13, 4649.
7. Davis, C. H.; Mathias, L. J.; Gilman, J. W.; Schiraldi, D. A.; Shields, J. R.; Trulove, P.; Sutto, T. E.; DeLong, H. J Polym Sci Part B: Polym Phys 2002, 40, 2661.
8. VanderHart, D. L.; Asano, A.; Gilman, J. W. Chem Mater 2001, 13, 3796.
9. Yoon, P. J.; Hunter, D. L.; Paul, D. R. Polymer 2003, 44, 5341.
10. Fornes, T. D.; Yoon, P. J.; Paul, D. R. Polymer 2003, 44, 7545.
11. Saujanya, C.; Imai, Y.; Tateyama, H. Polym Bull 2002, 49, 69.
12. Chang, J. H.; Kim, S. J.; Joo, Y. L.; Im, S. Polymer 2004, 45, 919.
13. Ke, I.; long, C.; Qi, Z. J Appl Polym Sci 1999, 71, 1139.
14. Pegoretti, A.; Kolarik, J.; Peroni, C.; Migliaresi, C. Polymer 2004, 45, 2751.
15. Suh, D. J.; Lim, Y. T.; Park, O. O. Polymer 2000, 41, 8557.
16. Barber, G. D.; Calhoun, B. H.; Moore, R. B. Polymer 2005, 46, 6706.
17. Solomon, O.; Ciuta, I. Z. J Appl Polym Sci 1962, 6, 683.
18. Berkowitz, S. J Appl Polym Sci 1984, 29, 4353.
19. Yoon, P. J.; Hunter, D. L.; Paul, D. R. Polymer 2003, 44, 5323.
20. Greene-Kelly, R. In The Differential Thermal Investigation of Clays; Mackenzie, R. C., Ed.; Mineralogical Society: London, 1957, pp 140.
21. Xie, W.; Gao, Z.; Lui, K.; Pan, W.-P., Vaia, R.; Hunter, D.; Singh, A. Thermochim Acta 2001, 367-368, 339.
22. Cui, L.; Khramov, D. M.; Bielawski, C. W.; Hunter, D. L.; Yoon, P. J.; Paul, D. R. Polymer 2008, 49, 3751.
23. Brophy, J. J.; Gallagher, M. J. Aust J Chem 1969, 22, 1405.
24. Calcagno, C. I. W.; Mariani, C. M.; Teixeira, S. R.; Mauler, R. S. Polymer 2007, 48, 966.